

Major and trace element abundances in the sand fractions of stream sediments from the Kando River, Shimane Prefecture, Japan

Edwin Ortiz* and Barry P. Roser*

Abstract

Hand-sieved sand fractions of 83 stream sediment samples from active channels of the Kando River system in the northern San-in district were analyzed by X-ray fluorescence for major elements and 14 trace elements. Histograms of individual elements generally display normal or positively skewed distributions, as is typical of stream sediments. Several elements (e.g. MgO, Fe₂O₃T, K₂O, Rb) have bimodal and polymodal distributions due to contrasting source proportions. There are clear differences in the compositions of sediments collected from secondary drainages upstream and downstream of the site of the Shitsumi dam. Those upstream are less aluminous, and tend to have greater abundances of K₂O, SiO₂, Ba, Ce, Nb, Pb, Rb, and Th than those downstream. In contrast, TiO₂, Fe₂O₃T, MgO, P₂O₅, Cr, Sc, Ni, V, and Y are generally more abundant in samples from below the dam site. These elemental associations and contrasts are directly related to source geology, as the catchment above the Shitsumi dam site is dominated by granitoids and felsic volcanic rocks, whereas that below consists of more mafic volcanic and sedimentary rocks of the Hata, Kawai-Kuri and Omori Formations. Intermediate compositions in the main channel in the lower reaches reflect mixing and obscuration of these two source signatures, although a geochemical fingerprint of a subordinate adakitic volcanic source (Mt. Sanbe) is also evident in this section of the river.

Key words: Geochemistry, Kando River, sand fraction, Shimane, stream sediments

Introduction

The study of element concentrations in stream sediments can play a significant role in the interpretation of natural processes in watersheds and the possible influence of human activity (Zhang and Wang, 2001). This paper reports X-ray fluorescence (XRF) analyses of the >180 μ m to < 2 mm fractions (hereafter, sand fractions) of 83 stream sediment samples collected from the catchment of the Kando River, east Shimane Prefecture. The Kando catchment is located SW of Izumo City, and has an area of about 448 km² (Fig. 1). Study of the characteristics of its sediments is relevant because a high dam is under construction at Shitsumi, in the middle reaches of the river. The dam will ultimately affect the sedimentation regime and composition of the sediments of the Kando River.

The aim of this report is to present the data obtained by XRF analysis, and to briefly outline the elemental abundances and variations in the sand fractions of sediments from the Kando River. The dataset described here complements an earlier report for the fine fractions (<180 μ m) of the same suite of samples (Ortiz and Roser, 2003). Collectively the analyses constitute representative baseline data for follow up-surveys in the Kando River in the future, and for comparative studies of other river systems in this part of the San-in region. More detailed examination of the results will be published later.

Geological Outline

In a simplified framework, the geology of the Kando River catchment is characterized by two sets of lithologies: Paleogene to Cretaceous granitoids and contemporaneous volcanic rocks south (upstream) of the Shitsumi dam site, and a more complex association of primarily Miocene rocks from the Kawai-Kuri, Omori, Hata, Matsue, and Fujina Formations downstream to the north (Fig. 1). Numerous workers have conducted studies of the units present in the area, including general geology, paleontology, stratigraphy, sedimentology, geochronology, and geochemistry (e.g. Takayasu, 1986; Kano *et al.*, 1989; 1991; 1994; 1997; Rezanov *et al.*, 1994; Morita and Nakayama, 1999; Iizumi *et al.*, 2000; Roser *et al.*, 2001). The granitoids in the southern part of the catchment include granites, granite porphyries, granodiorites, gabbros, quartz diorites, and tonalites, whereas the coeval volcanic rocks consist of rhyolite to dacite lavas and pyroclastic rocks, and lesser andesites (EBGMSP, 1997). In contrast, the lithotypes described in the northern part of the catchment comprise basaltic to rhyolitic lavas and pyroclastic rocks, mafic intrusives, and locally derived sedimentary rocks including sandstones, mudrocks, and conglomerates.

Other lithotypes crop out in the area to a lesser extent, including alkali basalt lavas, dolerites, porphyrites, and Sangun Group basic and psammitic schists. In addition, adakitic dacite lavas and pyroclastics originating from Mount Sanbe are supplied to the Kando River by several small tributaries in the west.

*Dept. of Geoscience, Shimane University, Matsue 690-8504, Japan

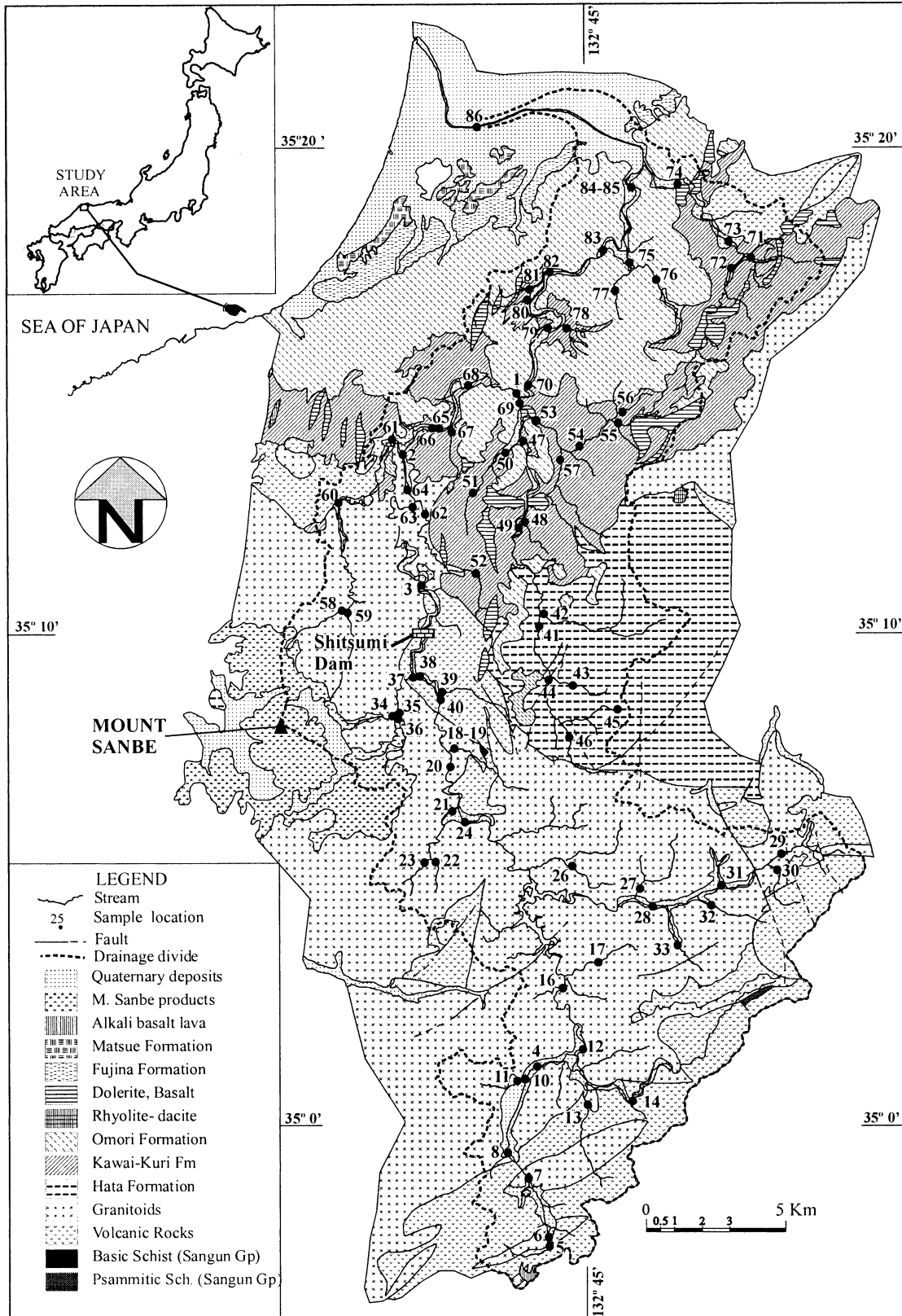


Fig. 1. Map showing the generalized distribution of lithotypes in the catchment of the Kando River and location of sample sites (after Ortiz and Roser, 2003). Geology based on the 1:200,000 geological map of Shimane Prefecture (Editorial Board of the Geological Map of Shimane Prefecture, 1997).

A marked contrast in source rock compositions thus exists between the areas above and below the dam site, in terms of both lithotype and chemistry. Hence, completion of the Shitsumi Dam will modify the composition of both suspended sediment (very fine sand to mud) and coarser bed load (coarse to fine sand) in the downstream reaches of the Kando River (Ortiz and Roser, 2003).

Sampling and Sample Preparation

1. Field sampling

A total of 86 samples were collected over eight days between September and November 2002. Weather was generally fine, and streams clear and low. Composite 1.0-1.5 kg samples were collected from active channels over lengths of 20-50 m. Choice of sampling sites was made using 1:50,000 topographic base maps overlain with geology from the 1:200,000 Geological map of Shimane Prefecture (EBGMSP, 1997). Site selection intended to survey representative drainages comprising the whole spectrum of lithologies present in the catchment. Locations of analyzed samples are given in Fig. 1, numbered in order of collection. Samples could not be taken at some intended sites due to the nature of the material present or to other factors, resulting in a spatial array slightly different than that originally planned. The range of source lithologies present was, however, completely covered. Overall sampling density was one sample/5.2 km².

2. Sample preparation

Once collected, the bulk samples were put into stainless steel trays and dried in a drying cabinet at 80-90°C. Each sample was then dry-sieved to remove material coarser than 2 mm. The <2 mm fraction was then split into quarters or eighths using a simple alumina chute, and then passed through an 83 mesh sieve to remove the <180 μm fraction. Part of the fraction retained in the 83 mesh sieve (sand fraction) was then crushed for about 30 seconds in a tungsten carbide ring mill in loads ranging between 50 and 150 g. From the crushed sub-samples, 7 to 10 g were transferred to glass vials and dried at 110°C for at least 24 hours prior to determination of loss on ignition (LOI). Three samples (K 9, K 15 and K 25) could not be analyzed, because the volume of the sand fraction was insufficient (<10 g in a half split). More detailed description of the field sampling and sample preparation are given in Ortiz and Roser (2003).

Analytical Methods

LOI was determined from the net weight loss of samples weighed before and after ignition in a muffle furnace at 1000°C for at least two hours. The ignited material was disaggregated in an agate pestle and mortar, and then held in an oven at 110°C for a minimum of 24 hours. Fusion

beads for XRF analysis (ignited basis) were prepared from this material, using an alkali flux (80 % lithium tetraborate and 20 % lithium metaborate) and a sample : flux ratio of 1:2, following the methods of Kimura and Yamada (1996).

Major elements expressed as oxides and 14 trace elements (Ba, Ce, Cr, Ga, Nb, Ni, Pb, Rb, Sc, Sr, Th, V, Y, Zr) were determined using a Rigaku RIX-2000 XRF at Shimane University. Analyses were monitored by comparison with the recommended values for seven GSI and USGS standards. More detail of the methods followed in this study is given by Roser *et al.* (2000, 2001) and Ortiz and Roser (2003).

Results and Discussion

XRF results for major and trace elements in the sand fractions are reported on a hydrous basis in Table 1. LOI contents were low (all <5 %), and are generally significantly less than those reported by Ortiz and Roser (2003) for the fine fractions in the same sample suite. There is also no clear association of the highest values with the samples collected from sites behind small dams or weirs, as seen in the fine fractions (Ortiz and Roser, 2003).

Elemental abundances in the sand fractions show significant variation even after normalization to 100% anhydrous to eliminate the effect of varying LOI (Table 2). The average composition over the entire suite is somewhat similar to that of average Upper Continental Crust (UCC), although most elements are slightly depleted. Greatest depletion is seen for Ni, Cr, Nb, and in the segment Mg-Ce, whereas V and Pb are slightly enriched (Fig. 2). The general depletion with respect to UCC is greater than that of the fine fraction average, which is enriched in Zr and the elements

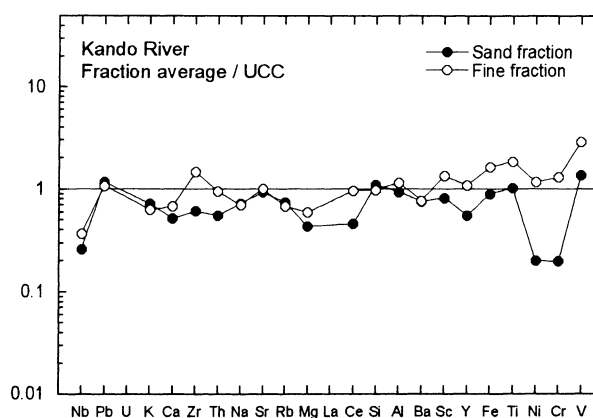


Fig. 2. Multi-element plot showing the average composition (anhydrous normalized) of the sand fractions from the Kando River (data from Table 2) normalized against the Upper Continental Crust (UCC) average of Taylor and McLennan (1985). Fine fraction (<180 μm) average from Ortiz and Roser (2003). Elements are arranged from left to right in order of increasing normalized abundance in average Mesozoic-Cenozoic greywacke (Condie 1993) relative to UCC, following the methodology of Dinelli *et al.* (1999). The major elements are normalized as oxides.

Major and trace element abundances in the sand fractions of stream sediments from
the Kando River, Shimane Prefecture, Japan

Table 1. Major and trace element analyses of the sand fractions, Kando River (hydrous basis). Major element values wt %, trace element values ppm.

SaNr	TYPE	SiO ₂	TiO ₂	Al ₂ O ₃	Fe ₂ O ₃ T	MnO	MgO	CaO	Na ₂ O	K ₂ O	P ₂ O ₅	LOI	SUM	Ba	Ce	Cr	Ga	Nb	Ni	Pb	Rb	Sc	Sr	Th	V	Y	Zr	% Sand
K1	MCB	74.07	0.39	12.91	3.38	0.09	0.95	2.43	2.78	2.14	0.08	1.25	100.47	375	22	22	15	6	5	22	88	6.8	320	3.6	60	10	102	96.5
K2	MCB	69.84	0.66	13.90	5.76	0.10	0.96	2.53	3.04	2.45	0.08	1.15	100.48	394	30	20	17	8	5	26	83	6.4	419	6.5	131	10	112	87.1
K3	MCB	70.98	0.33	14.87	2.81	0.07	0.85	2.71	3.13	2.64	0.08	1.82	100.29	394	34	8	16	7	2	23	94	3.2	467	7.7	39	10	95	70.0
K4	A	75.38	0.31	12.43	2.93	0.08	0.56	1.55	2.42	3.22	0.05	1.28	100.22	445	31	3	14	6	1	20	116	1.7	214	5.1	35	10	90	90.7
K5	A	70.13	1.44	12.18	8.56	0.17	0.73	1.02	0.85	2.81	0.06	2.41	100.37	400	42	34	17	14	14	23	125	8.8	133	11.1	248	16	244	93.9
K6*	A	73.84	0.47	13.57	3.71	0.08	0.56	0.84	0.82	3.22	0.05	3.17	100.33	437	38	15	17	10	12	25	148	6.9	128	10.3	68	13	163	92.1
K7	A	76.51	0.53	11.20	3.77	0.10	0.54	1.25	1.88	3.26	0.05	1.36	100.45	400	29	2	13	8	2	19	125	4.9	170	8.0	66	12	109	84.7
K8	A	78.42	0.20	11.23	2.17	0.08	0.42	0.82	1.50	3.79	0.04	1.47	100.14	475	24	3	11	5	1	22	144	3.5	124	6.8	9	10	80	93.0
K10	A	79.30	0.22	10.45	2.47	0.08	0.47	1.38	2.06	2.74	0.05	0.95	100.17	405	26	0	12	4	1	19	102	1.7	182	6.1	25	10	93	90.9
K11	A	75.52	0.36	11.35	4.84	0.10	0.58	1.34	2.30	2.97	0.03	1.12	100.50	452	33	5	13	5	2	17	103	5.5	195	6.0	74	9	130	91.9
K12	A	78.72	0.30	11.09	2.54	0.08	0.58	1.39	2.10	2.98	0.04	1.05	100.87	429	29	0	12	5	1	20	105	4.1	187	4.8	38	9	82	95.0
K13*	A	83.42	0.10	8.62	0.98	0.03	0.31	0.41	1.17	3.82	0.02	0.70	99.58	696	21	0	8	3	0	18	122	0.5	80	5.9	2	5	48	91.9
K14	A	74.06	0.41	12.91	2.94	0.07	0.61	1.44	2.56	3.50	0.04	1.58	100.13	440	20	1	14	8	2	30	126	5.6	202	7.7	49	13	109	85.1
K16	A	75.99	0.44	11.78	3.18	0.07	0.56	1.48	2.43	3.24	0.05	1.07	100.28	438	17	1	11	5	1	22	114	3.2	188	5.4	56	10	80	96.0
K17	A	70.37	0.35	15.16	3.13	0.08	0.75	1.82	2.95	3.72	0.04	2.00	100.36	471	13	1	16	7	3	24	143	5.7	300	9.3	30	10	113	89.6
K18	A	69.03	0.87	12.15	8.63	0.15	1.19	2.28	2.66	2.18	0.08	0.89	100.39	301	27	31	17	9	6	42	89	9.5	260	8.3	264	18	134	92.2
K19	A	74.48	0.29	13.48	2.53	0.10	0.74	1.61	2.12	2.87	0.04	1.86	100.10	341	40	3	15	8	9	71	124	5.3	276	10.5	28	14	119	94.3
K20	A	72.16	0.37	14.18	3.26	0.11	0.83	2.35	3.22	2.70	0.06	1.22	100.47	404	39	5	14	7	3	28	99	4.9	410	7.4	45	9	110	92.3
K21	A	73.06	0.34	13.59	3.31	0.13	0.78	1.95	2.70	2.48	0.08	1.64	100.04	398	43	2	15	7	0	31	89	5.5	346	4.6	37	10	126	90.0
K22	A	72.79	0.40	13.36	3.51	0.18	0.81	2.14	2.76	2.34	0.07	1.66	100.04	406	60	1	16	7	2	24	80	7.6	382	6.4	37	10	138	89.7
K23	A	71.29	0.32	14.70	2.65	0.11	0.74	1.96	3.56	3.07	0.06	1.52	99.99	418	25	2	16	7	1	29	119	7.3	326	6.1	27	12	106	90.8
K24	A	69.76	0.33	15.16	3.17	0.09	0.69	1.77	3.61	3.64	0.06	1.74	100.02	422	43	6	17	9	2	19	142	6.8	244	9.9	20	16	128	84.1
K26	A	68.56	0.30	16.22	3.18	0.10	0.71	1.85	3.75	3.46	0.05	2.00	100.19	487	41	2	19	7	2	18	128	6.4	346	9.2	26	11	103	94.8
K27	A	72.39	0.45	12.98	4.92	0.11	0.65	1.63	2.91	2.97	0.04	1.18	100.23	460	18	4	14	6	2	19	94	3.4	290	6.7	70	8	112	93.6
K28	A	74.04	0.29	13.21	2.91	0.09	0.61	1.44	3.52	3.09	0.05	0.98	100.23	468	38	5	14	7	2	16	116	7.9	216	7.5	32	13	101	98.7
K29*	A	71.05	0.35	14.11	3.09	0.12	0.80	1.98	2.93	2.89	0.06	2.61	99.99	476	37	0	16	7	4	34	92	5.9	315	7.1	50	11	112	84.3
K30	A	72.61	0.34	13.78	2.79	0.10	0.67	1.44	3.19	3.08	0.06	1.89	99.96	481	37	3	16	9	2	25	101	6.2	247	7.0	44	16	166	91.8
K31*	A	75.60	0.27	12.21	2.60	0.08	0.61	1.43	2.54	2.98	0.05	1.48	99.84	456	30	3	14	6	2	20	102	5.0	229	6.2	30	10	95	94.6
K32	A	74.89	0.31	12.55	2.94	0.09	0.65	1.85	2.82	2.81	0.04	1.16	100.10	420	38	9	14	5	2	20	88	6.4	278	6.0	43	10	100	97.7
K33	A	73.82	0.26	13.36	2.43	0.06	0.64	0.71	2.87	3.41	0.03	1.29	98.88	481	22	4	15	5	2	23	110	6.1	276	5.4	27	8	82	95.1
K34*	A	67.01	0.29	16.61	3.13	0.10	1.30	4.34	4.09	1.77	0.11	0.69	99.44	445	36	8	19	7	5	16	50	5.8	815	5.2	37	6	94	98.7
K35*	A	66.44	0.26	17.20	2.71	0.09	1.16	4.43	4.23	1.78	0.10	0.96	99.34	435	29	4	18	8	4	20	52	6.5	853	5.8	24	6	85	78.5
K36*	A	66.70	0.26	16.94	2.80	0.08	1.20	4.41	4.33	1.77	0.09	0.55	99.14	459	36	3	19	7	7	16	48	6.0	866	5.0	32	6	86	95.9
K37*	A	67.47	0.27	17.10	2.72	0.09	1.12	4.44	4.22	1.71	0.10	0.69	99.93	418	29	2	19	7	6	17	50	6.5	828	5.0	28	7	85	97.7
K38	A	72.43	0.45	13.52	3.69	0.12	0.82	2.17	3.02	2.80	0.05	1.25	100.12	388	27	2	16	7	3	27	100	6.1	358	6.4	69	11	125	90.7
K39	A	71.13	0.49	14.44	3.88	0.11	0.79	1.73	2.33	2.80	0.04	2.40	100.14	449	35	5	17	8	4	47	105	6.5	303	8.4	74	10	139	88.1
K40	A	73.68	0.28	13.46	2.42	0.09	0.72	2.00	3.14	2.80	0.05	1.16	99.80	393	24	6	15	5	1	26	106	4.1	347	7.3	31	10	100	92.3
K41	B	68.73	0.53	14.35	5.40	0.15	1.32	2.48	2.49	2.35	0.07	2.21	100.07	373	25	2	17	5	3	21	82	15.4	311	4.9	108	14	102	88.8
K42	B	66.72	0.59	16.21	5.63	0.15	1.11	2.27	2.07	1.98	0.07	3.35	100.14	390	22	8	19	6	6	23	63	15.7	306	5.5	121	13	128	93.6
K43	B	64.70	0.64	17.51	5.36	0.15	1.07	2.18	2.22	1.62	0.08	4.80	100.31	394	38	8	19	6	5	23	55	14.6	385	5.8	102	13	128	66.0
K44	B	69.24	0.39	14.84	4.28	0.13	1.09	2.21	2.61	3.05	0.05	2.16	100.06	418	25	3	17	6	4	23	107	12.4	325	5.6	75	11	102	95.4
K45*	B	65.89	0.50	17.78	4.06	0.10	0.98	2.56	2.89	1.83	0.07	3.70	100.35	419	25	6	19	7	3	18	54	11.2	488	7.0	67	12	138	84.8
K46	B	70.73	0.23	15.04	2.34	0.08	0.60	1.74	2.96	4.62	0.03	1.36	99.74	420	18	3	17	8	2	27	167	6.5	317	6.5	22	10	87	94.4
K47	B	69.12	0.55	14.53	5.35	0.13	1.17	1.97	2.68	2.06	0.09	2.68	100.33	348	30	3	16	5	4	19	67	14.3	261	4.4	97	16	126	94.0
K48	B	67.69	0.81	14.41	7.22	0.16	1.19	1.20	2.63	1.60	0.11	3.49	100.51	345	26	20	17	5	9	16	51	14.3	176	5.7	144	18	155	84.3
K49	B	68.71	0.54	15.15	5.18	0.11	1.16	2.06	2.36	2.12	0.07	2.86	100.32	371	22	6	18	5	6	20	70	15.5	287	5.1	94	13	118	96.1
K50	B	66.53	0.85	14.10	6.88	0.15	1.14	1.66	2.52	1.61	0.09	2.90	100.44	333	35	12	17	6	8	19	52	15.9	194	6.1	116	20	149	94.6

SaNr	TYPE	SiO ₂	TiO ₂	Al ₂ O ₃	Fe ₂ O ₃ T	MnO	MgO	CaO	Na ₂ O	K ₂ O	P ₂ O ₅	LOI	SUM	Ba	Ce	Cr	Ga	Nb	Ni	Pb	Rb	Sc	Sr	Th	V	Y	Zr	% Sand
K51	B	69.66	0.67	14.14	5.69	0.15	1.17	1.87	2.71	1.63	0.09	2.61	100.41	316	25	3	16	6	1	14	51	13.0	197	3.7	99	20	145	92.8
K52	B	68.48	0.74	14.85	6.22	0.17	0.91	1.71	2.27	1.87	0.08	3																

Table 2. Summary statistics for all sand fraction samples (anhydrous normalized data). N= 83.

Element	Mean	Min	Max	SDp
<i>Major elements (wt %)</i>				
SiO ₂	72.31	66.63	84.37	3.31
TiO ₂	0.50	0.10	1.47	0.25
Al ₂ O ₃	14.21	8.72	18.40	1.76
Fe ₂ O ₃	4.45	0.99	9.20	1.78
MnO	0.11	0.03	0.19	0.03
MgO	0.94	0.31	2.12	0.29
CaO	2.16	0.42	4.50	0.82
Na ₂ O	2.80	0.85	4.39	0.67
K ₂ O	2.45	1.13	4.70	0.69
P ₂ O ₅	0.07	0.02	0.12	0.02
<i>Trace elements (ppm)</i>				
Ba	410.1	285.3	703.4	56.1
Ce	29.3	13.6	61.1	8.0
Cr	6.9	0.0	34.9	7.0
Ga	16.0	7.6	20.3	2.1
Nb	6.4	3.1	13.8	1.6
Ni	4.0	0.0	14.4	2.7
Pb	23.0	12.1	71.9	8.0
Rb	82.9	25.9	170.1	30.8
Sc	9.0	0.5	20.8	4.5
Sr	324.9	81.2	878.8	171.4
Th	5.8	2.4	11.3	1.8
V	81.1	2.0	276.4	55.6
Y	11.9	4.9	20.4	3.4
Zr	114.6	49.0	248.8	26.9
Min	Minimum			
Max	Maximum			
SDp	Population standard deviation			

significant divergence, with tendency to polymodal distributions.

Among the trace elements, Ga (Fig. 4a), Ba, Ce, Th and to some extent Zr have somewhat normal distributions, although all contain a few anomalous values. The rest of the trace elements analyzed have more irregular distributions, with wide variations in their contents and marked skew. Strong skew to higher values is especially shown by Cr (Fig. 4b), Ni, Pb, Sr, and V. Several other elements (Nb, Rb (Fig. 4c), Sc (Fig. 4d) and Y) show moderate to clear polymodal patterns.

The results for the sand fractions from the Kando River thus generally show normal right-skewed distributions, and as such are typical of fractions taken from stream sediments. Most of the elements analyzed are not prone to disturbance caused by human activity, and there is no clear evidence of exceptional values of potentially sensitive elements such as Ni or Pb (metallic sources) or P₂O₅ (from fertilizer). Consequently, we consider the compositions observed are chiefly related to those of the source rock types, and to the soils derived from them. Sporadic anomalous or elevated values of elements including Fe, Mn, Ti, Ce, Cr, Ni, Th, V, Y and Zr, also described by Ortiz and Roser (2003) for the fine fraction, are most likely due to concentration of high density accessory minerals, textural immaturity, and short

transport distance.

Bimodal and/or polymodal distributions of several elements (e.g., Al, Mg, K, Rb, Sc; Figs 3 and 4) may reflect the control exerted by source rock composition. As outlined above, two main groups of lithotypes occur in the catchment of the Kando River. The first is mainly felsic (granitoids and volcanic rocks) and is located south of the Shitsumi Dam, whereas the second consists of more mafic rocks of the Hata, Kawai-Kuri, and Omori Formations to the north of the dam site. To evaluate the influence of source rocks, the sample sites were divided into three categories, following Ortiz and Roser (2003):

- (1). Sites above the dam site (all sites upstream of site 3)
- (2). Main channel sites below the dam site (3, 63, 64, 2, 66, 65, 68, 1, 79, 82, 83, 84-86).
- (3). Secondary drainages below the dam site.

Significant contrasts in the chemistry of samples from the different categories are evident on simple element-Al₂O₃ variation diagrams. In the major elements, fractions derived from felsic sources from above the dam site tend to be less aluminous (<16 wt %) than those in the main channel or from the secondary drainages below the dam site, except for sample K 26 and a group of samples (K 34-37) collected from tributaries with headwaters in the Mount Sanbe area (Fig. 5). This contrasts with the <180 μm fractions, which tend to be more aluminous (>17 wt %) above the Shitsumi dam site than below (Ortiz and Roser, 2003). This suggests compositional dependence related to clast size and source, with greater abundances of quartz and feldspar in the sand fractions of samples derived from the felsic rocks, and concentration of clays in the fine fractions.

Excluding Na₂O (Fig. 5a) and MnO, which show little contrast between the categories, the remaining major elements all display some distinction between the three groups, although overlap is significant. K₂O (Fig. 5b) and to a lesser extent SiO₂ have greater contents in samples from above Shitsumi, although samples originating from Mount Sanbe plot are clearly lower with respect to the other samples in this category. In contrast, CaO (Fig. 5c) is generally least abundant in samples from above the dam site, although Sanbe-derived samples K 34-37 have markedly higher values than the rest of the entire suite. In general, TiO₂ (Fig. 5d), Fe₂O₃T, MgO, and P₂O₅ abundances are greatest in samples derived from the more mafic rocks in the secondary drainages below the dam site. Samples from the main channel below site 3 are intermediate in K₂O, P₂O₅, MgO, and to some degree in SiO₂ and TiO₂, whereas CaO and Na₂O abundances tend to plot in the upper part. Abundances of MnO and Fe₂O₃T in this category show considerable scatter.

Contrasts between the groups are also evident among the trace elements. Ba (Fig. 6a), Ce, Rb, Th, and to an extent Nb and Pb are clearly more abundant in the fractions from above the dam site. This elemental association is compatible

Major and trace element abundances in the sand fractions of stream sediments from the Kando River, Shimane Prefecture, Japan

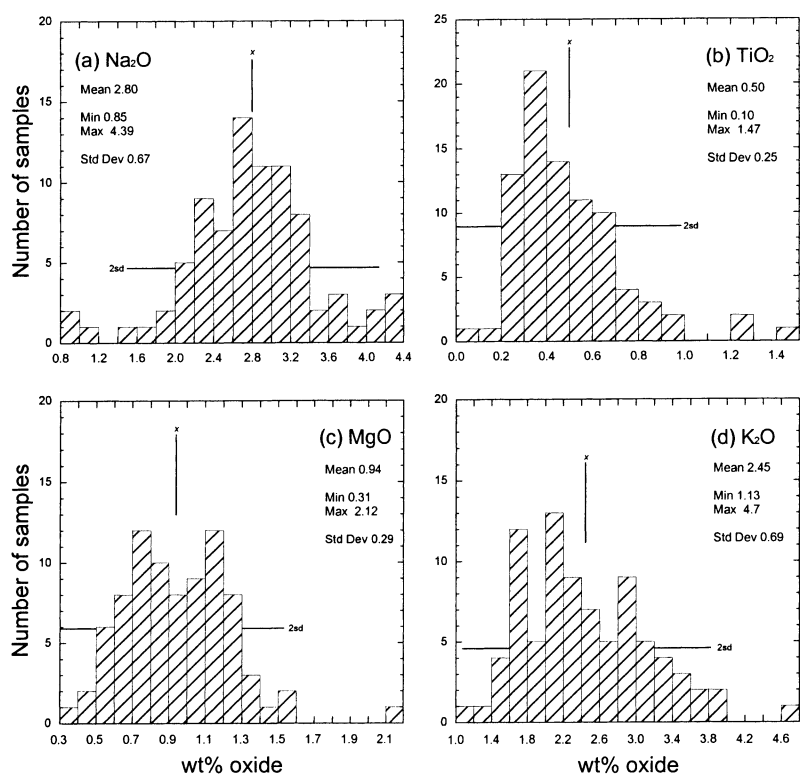


Fig. 3. Examples of histograms of major element abundances (anhydrous normalized data) in the sand fraction, Kando River. Min = minimum; Max = maximum; Std Dev = standard deviation; vertical bar x = mean; horizontal bar ($2sd$) = ± 2 standard deviations from the mean. (a) Na_2O - normal distribution, skewed to lower values; (b) TiO_2 - skewed to higher values; (c) MgO - bimodal; (d) K_2O considerable variation, with tendency for polymodality.

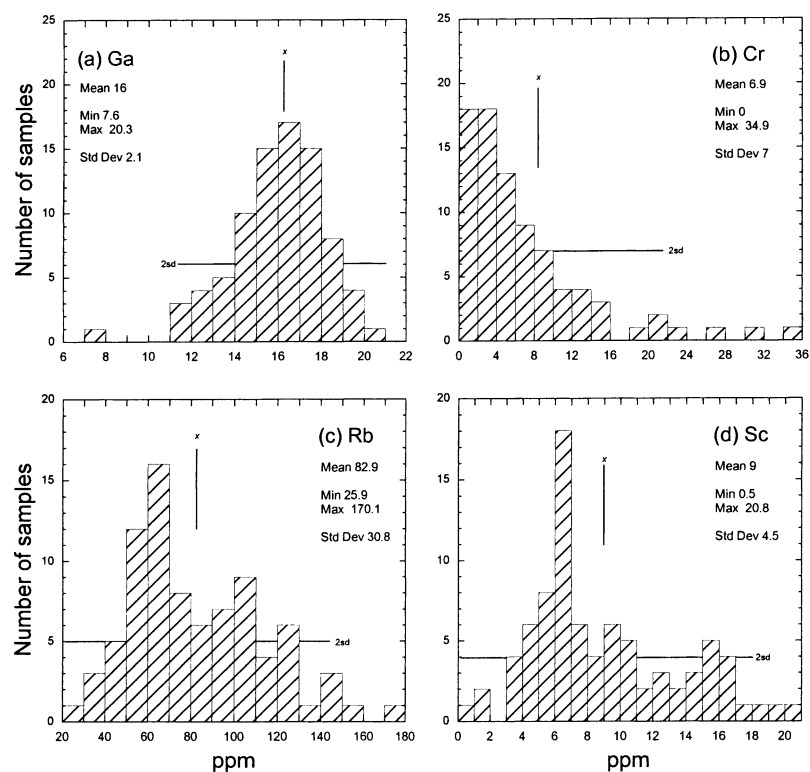


Fig. 4. Examples of histograms of trace element abundances (anhydrous normalized data) in the sand fraction, Kando River. Min = minimum; Max = maximum; Std Dev = standard deviation; vertical bar x = mean; horizontal bar ($2sd$) = ± 2 standard deviations from the mean. (a) Ga - relatively normal; (b) Cr - strongly skewed to higher values; (c) Rb and (d) Sc - moderate to clear polymodal patterns.

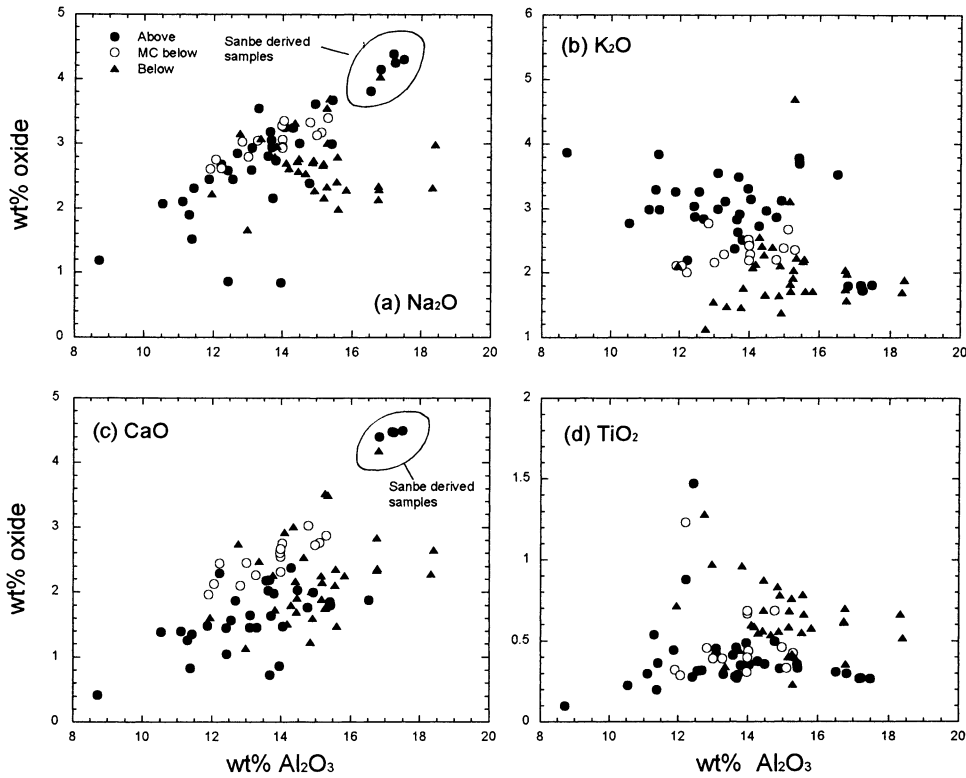


Fig. 5. Examples of major element- Al_2O_3 variations in the sand fractions (anhydrous normalized data), Kando River, according to position with respect to the dam site. MC below = main channel below the dam site. (a) Na_2O - little difference between groups; (b) K_2O - greater abundances in samples from above the dam site; (c) CaO - lower values in samples from above, greater in samples from the main channel below; (d) TiO_2 - greater abundances in samples from secondary catchments below the dam site.

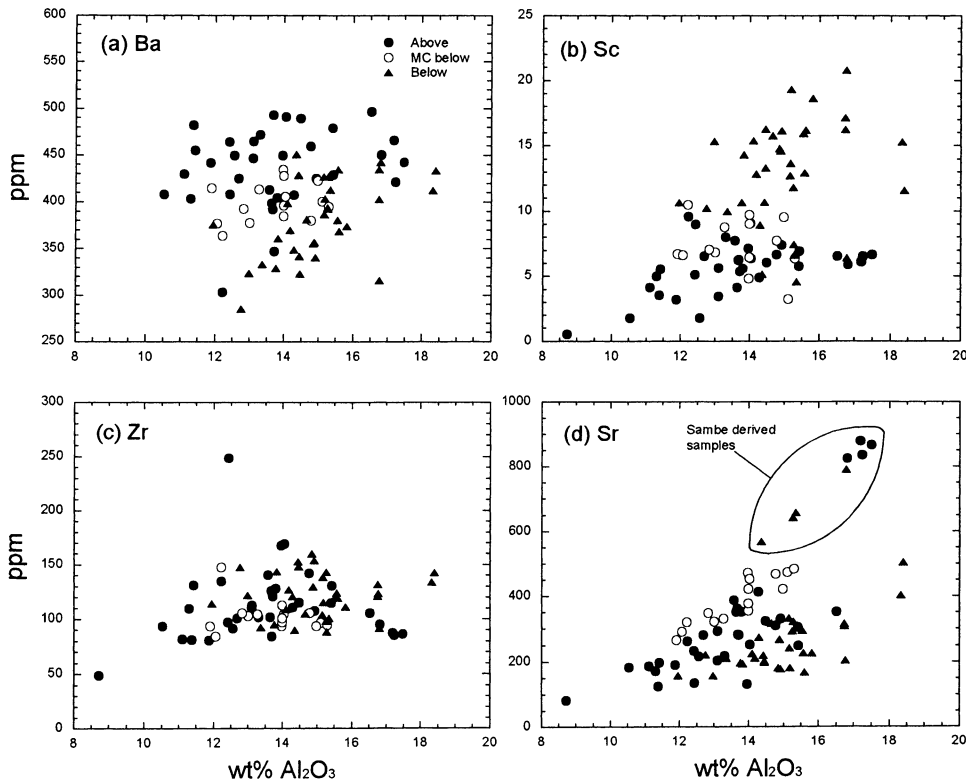


Fig. 6. Examples of trace element- Al_2O_3 variations in the sand fractions (anhydrous normalized data), Kando River, according to position with respect to the dam site. MC below = main channel below the dam site. (a) Ba - greater abundances in samples from above the dam site; (b) Sc - greater abundances in samples from secondary catchments below the dam site; (c) Zr - little difference between groups; (d) Sr - greater abundances in samples from the lower main channel. Circled samples from secondary drainages (K 34-37; 58-61) are derived directly from Mt Sanbe.

with the felsic source rocks (granitoids and felsic volcanics rocks) present in the area. Contents of Sc (Fig. 6b) and V are markedly greater in samples from the secondary drainages below Shitsumi, with almost no overlap with the fractions derived from felsic sources. Abundances of Cr, Ni and Y also tend to be higher in the group below the dam site, reflecting the more mafic nature of the source lithotypes in this part of the catchment. Little contrast is observed between the three categories for Zr (Fig. 6c) and Ga.

Although overlap is considerable, abundances of most trace element in samples from the main channel below the dam site are intermediate to those from above and below. This reflects mixing in the main channel in the lower reaches of the Kando River of detritus supplied mainly from two areas with differing source compositions (felsic to the south and more mafic to the north), and consequent suppression of the primary source signatures. Strontium, however, is an exception. Sr abundances in the main channel fractions are greater than the majority of fractions from the smaller drainages both above and below Shitsumi (Fig. 6d). However, eight samples (K 34-37; 58-61) from the latter two groups have significantly greater Sr concentrations (500-900 ppm) than the lower main channel fractions. All eight samples were collected from two streams that drain directly off Mt Sanbe (Fig. 1), and their chemistry is clearly influenced by Sr-rich adakitic dacite detritus from that source. This provenance fingerprint is retained in the fractions in the main channel below the dam site, despite dilution from other source lithotypes. This is also apparent for CaO and Na₂O, though less clearly (Fig. 5). A similar pattern is evident in the fine fraction data reported by Ortiz and Roser (2003), although overlap of the lower main channel fractions with the secondary drainages is a little greater. However, the compositions of both fractions record source rock signatures. Comparison between the results for the two fractions will be discussed further in future work.

Conclusions

Bulk chemical compositions of sand fractions of sediments from the Kando River and subsidiary drainages correspond in general with the nature of their source rocks and derived soils. Significant differences in the chemical compositions of sediments reveal clear influence of either felsic (granitoids and volcanic rocks) or more mafic (Hata, Kawai-Kuri and Omori Formations) source lithotypes with respect to the spatial location of samples. Isolated high values for individual elements likely reflect local concentrations of high-density accessory minerals. Intermediate compositions in samples from the main channel in the lower reaches of the Kando River reflect mixing and homogenization of this detritus. However, adakitic source signatures from Mt Sanbe are retained in the

lower reaches, despite dilution from the felsic and more mafic source rocks that form the majority of the catchment.

Acknowledgements

This work was part of a collaborative project with the Tokuo Laboratory for Study of Brackish Water Environments, Matsue. Our thanks to Takao Tokuo for suggesting the project and for facilitating it, and to Masami Saito (Tokuo Laboratory) for her help with administration. We are also grateful to Miwa Akashi and Minoru Oono of Takeshita Engineering Consultant Co. for their invaluable assistance during fieldwork.

References

- Condie, K. C., 1993, Chemical composition and evolution of the upper continental crust: Contrasting results from surface samples and shales. *Chem. Geol.*, **104**, 1-37.
- Dinelli, E.; Lucchini, F.; Mordenti, A. and Paganelli, L., 1999, Geochemistry of Oligocene-Miocene sandstones of the northern Apennines (Italy) and evolution of chemical features in relation to provenance changes. *Sed. Geol.*, **127**, 193-207.
- Editorial Board of Geological Map of Shimane Prefecture (EBGMSP) 1997. Geological map of Shimane Prefecture (1:200,000).
- Iizumi, S., Imaoka, T. and Kagami, H., 2000, Sr-Nd isotope ratios of gabbroic and dioritic rocks in a Cretaceous-Paleogene granite terrain, Southwest Japan. *The Island Arc*, **9**, 113-127.
- Kano, K., Matsuura, H., Sawada, Y., and Takeuchi, K., 1997, *Geology of the Iwami-Oda and Oura districts. With geological sheet map at a scale of 1:50,000*. Tsukuba, Geological Survey of Japan, 118 p.*
- Kano, K., Takeuchi, K., and Matsuura, H., 1991, *Geology of the Imaichi district. With geological sheet map at a scale of 1:50,000*. Tsukuba, Geological Survey of Japan, 79 p.*
- Kano, K., Takeuchi, K., Oshima, K. and Bunno, M., 1989, *Geology of the Taisha district. With geological sheet map at a scale of 1:50,000*. Tsukuba, Geological Survey of Japan, 30 p.*
- Kano, K., Yamauchi, S., Takayasu, K., Matsuura, H. and Bunno, M., 1994, *Geology of the Matsue district. With geological sheet map at a scale of 1:50,000*. Tsukuba, Geological Survey of Japan, 126 p.*
- Kimura, J.-I. and Yamada, Y., 1996, Evaluation of major and trace element analyses using a flux to sample ratio of two to one glass beads. *Jour. Mineral. Petrol. Econ. Geol.*, **91**, 62-72.
- Morita, H. and Nakayama, K., 1999, Stratigraphy of the Middle Miocene in southwestern part of Izumo City in Shimane Prefecture of SW Japan, and subsiding properties of its sedimentary basin. *Geosci. Rep. Shimane Univ.*, **18**, 25-39.*
- Ortiz, E. and Roser, B.P., 2003, Major and trace element abundances in the <180 μm fractions of stream sediments from the Kando River, Shimane Prefecture, Japan. *Geosci. Rep. Shimane Univ.*, **22**, 111-120.
- Potter, P.E., 1978, Petrology and chemistry of modern big river sands. *Jour. Geol.*, **86**, 423-449.
- Rezanov, A., Kagami, H. and Iizumi S., 1994, Rb-Sr isochron ages of Cretaceous-Paleogene granitoid rocks in the central part of the Chugoku district, southwest Japan. *Jour. Geol. Soc. Japan*, **100**, 651-657.
- Roser, B.P., Kimura, J.-I. and Hisatomi, K., 2000, Whole-rock elemental abundances in sandstones and mudrocks from the Tanabe Group, Kii Peninsula, Japan. *Geosci. Rep. Shimane Univ.*, **19**, 101-112.
- Roser, B.P., Tateishi, Y. and Nakayama, K., 2001, Whole-rock geochemical compositions of Miocene sedimentary and volcanic rocks from the Izumo - Matsue districts and Shimane Peninsula, SW Japan. *Geosci. Rep. Shimane Univ.*, **20**, 69-82.
- Takayasu, K., 1986, Diversification in the molluscan fauna of the Miocene Izumo Group, San-in district, southwest Japan. *Paleont. Soc. Japan, Spec.*

Pap., **29**, 173-186.

Taylor, S.R., and McLennan, S.M., 1985, *The continental crust: its composition and evolution*. Blackwell Scientific, Oxford, 312 p.

Zhang, C. and Wang, L., 2001, Multi-element geochemistry of sediments

from the Pearl River System, China. *Applied Geochem.*, **16**, 1251-1259.

* In Japanese, English abstract or summary

(Received: Oct. 20, 2004, Accepted: Nov. 28, 2004)

(要 旨)

E. Ortiz · B.P. Roser, 2004, 島根県, 神戸川の河川堆積物の砂部分の主成分, 微量成分組成. 地球資源環境学科学研究報告, **23**, 17-25

山陰地方北部, 神戸川水系の現河床から得た 83 の堆積物試料について篩いを用いて砂部分だけを取り出し, その試料について XRF 分析結果を基に, 主成分元素と 14 の微量成分元素の解析を行った. 各元素のヒストグラムは, 通常の河川堆積物に見られるように, 対称な分布または正の方向にゆがんだ分布を示す. いくつかの元素 (例えば, MgO, Fe₂O₃T, K₂O, Rb) は, 供給源の割合を反映して, 二峰性または多峰性の分布を示す. 志津見ダムの上流と下流の 2 次支流からのサンプルの組成にははっきりとした違いが見られた. ダムよりも上流のものはアルミニウムに乏しく, K₂O, SiO₂, Ba, Ce, Nb, Pb, Rb, Th が下流のものよりも多く含まれる傾向が見られた. それに対して, TiO₂, Fe₂O₃T, MgO, P₂O₅, Cr, Sc, Ni, V, Y については一般的にダムサイトよりも下流からの試料に多く含まれる. これらの元素の組み合わせならびに違いは供給源の地質に直接的に関係する. それは志津見ダムよりも上流の集水域には花崗岩類やフェルシクな火山岩が分布をするのに対して, 下流では波多, 川合-久利, 大森層のよりマフィックな火山岩ならびに堆積岩が分布をするためである. 従属的な要素である三瓶山起源のアダカイト質火山岩からの化学物質の痕跡があるにもかかわらず, 主要流路のより下流では中間的な組成が見られた. それは, 堆積物が混合し, 2 つの供給源が曖昧にされていることを反映している.